

Chapter 8. SLH Performance and Design Principles

8.1 Introduction

In this chapter we examine the performance of the Stub Loaded Helix in light of some of the results presented in the preceding chapters. Specifically, we compare the performance of the SLH to previously reported results for the full size axial mode helix and examine the size reduction achieved by the SLH for comparable gain performance. We also compare the results of measurements with simulation results presented in earlier. Lastly, based on the simulation and measurement results, we present a set of design parameters for an SLH for maximized gain, axial ratio bandwidth, and size reduction.

8.2 The Gain of the SLH

An important question is how does the gain and axial ratio performance of the Stub Loaded Helix compare to the full size axial mode helix. The classic measurement study on helices was performed by King and Wong [1980]. Their work produced a large number of parametric curves that describe the gain performance of helices with respect to axial length, pitch angle, and circumference. Figure 8.1 is from King and Wong's paper and shows the measured gain versus frequency for a various helices with 5 to 35 turns.

Two horizontal reference lines have been added to Figure 8.1 to represent the average gains across the operational (axial ratio) bandwidths of the 5- and 10-turn SLH antennas modeled in Sections 5.3 and 5.4. This comparison is based purely on the gain and number of turns of each of the antennas and does not account for any differences in size or operating frequency or bandwidth. The average gain is used as a typical performance parameter for the SLH since the variation in gain of the SLH across its operational bandwidth is relatively small. From Figures 5.4 and 5.8, we can see that the gain variation across the operational bandwidth is typically no more than 2 dB for the 5- and 10-turn SLHs modeled.

The intersection of the SLH reference lines with the corresponding gain curve for the appropriate number of turns provides a comparison between the gain performance of the SLH and the full size helix. In both cases the gain of the SLH is approximately 2.5 dB below the *peak* gain of the full size helix as measured by King and Wong. King and Wong's measurements did not include axial ratio performance data so that operational bandwidth could be evaluated. But, based on the diameter of their test article (4.23 inches) given in Figure 8.1, we assume that the nominal center frequency of operation would be 888 MHz for f_c occurring at $C = 1\lambda = 13.29$ inches = 33.75 cm. Since the peak gains shown in Figure 8.1 occur significantly above this nominal center frequency, the gain comparison to the full size helix with the SLH is actually better than first assumed.

For the 5-turn curve in Figure 8.1, the full size helix gain at $C = 1\lambda$ is approximately 9.8 dB, compared to an average gain of 8.5 dB for the 5-turn SLH. For the 10-turn curve in Figure 8.1, the full size helix gain is 12 dB at $C = 1\lambda$. The corresponding average gain of the SLH is 10.5 dB. The gain of the SLH antennas compares favorably with the full size helix, especially when the difference in sizes is considered.

Let us compare the SLH and the full size helix dimensions for equal gains, using the curves in Figure 8.1. If we take the frequency at which the SLH gain line intersects the corresponding helix gain curve in Figure 8.1 and use that wavelength to normalize the helix dimensions in terms of wavelengths, we can compare the sizes of the corresponding helices. For the 5-turn case, the full size helix exhibits the same gain as the SLH at 790 MHz. At 790 MHz, the circumference of the full size helix is 0.8888λ . Referring to Figures 5.4 and 5.5, the lower usable frequency of the 5-turn SLH modeled is 210 MHz. The circumference of the modeled SLH at 210 MHz is 0.70λ . The circumferential reduction from 0.8888λ to 0.70λ is 21.2% for the SLH versus the full size helix for the same gain.

There is an even greater size reduction if the length of the antennas are considered. Given the pitch and circumference specified in Figure 8.1, a 5-turn helix would be 1.013λ long at 790 MHz. The equivalent 5-turn SLH is only 0.492λ long. This is a 51.4% reduction in length for the SLH compared to the full size helix. The reduction in length of the SLH is due not only to the smaller circumference but also the smaller pitch angle of the SLH.

Similar calculations can be made for the 10-turn helices of equal gain using 810 MHz for the full size helix and 195 MHz for the SLH modeled above. The results are shown in Table 8.1 for both 5- and 10-turn helices.

The length and diameter reductions can be used to calculate the volume reduction achieved by the SLH. Table 8.1 shows the normalized circumferences and lengths and the normalized volume. Both 5- and 10-turn SLH antennas have volumes on the order of at least 70% less than the conventional helices. At VHF and UHF frequencies where helices become physically large, this reduction in volume can translate into a significant reduction in wind loading for the antenna. The smaller wind load for the antenna permits smaller support structures that reduces total weight and costs.

**Table 8.1 Comparison of Dimensions of Full Size Helix and SLH Antennas
From Figure 8.1 and NEC Models**

	Full Size Helix	Stub Loaded Helix	Size Reduction
5-Turn		Model M5-1,2	
Circumference	0.8888 λ	0.7000 λ	21.2%
Length	1.013 λ	0.492 λ	51.4%
Volume	0.0637 λ^3	0.0192 λ^3	69.9%
10-Turn		Model M10-1,2	
Circumference	0.9112 λ	0.6500 λ	28.6%
Length	2.078 λ	0.9135 λ	56%
Volume	0.1373 λ^3	0.0307 λ^3	77.6%

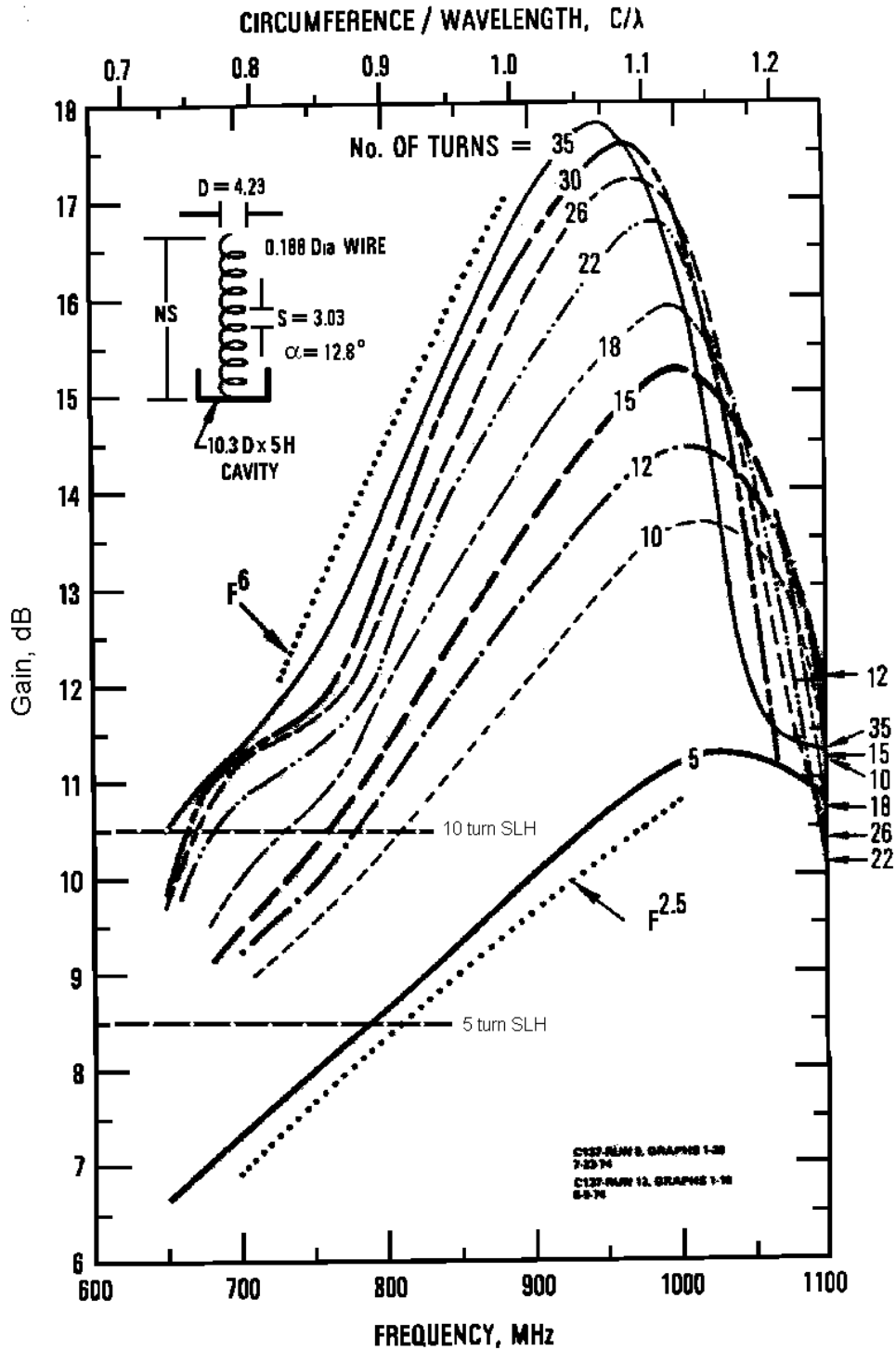


Figure 8.1 Antenna gain versus frequency for 5- to 35-turn helical antennas, 4.23-in diameter. The curves are from [King and Wong, 1980]. The horizontal dashed lines indicated average SLH gains for 5- and 10-turn models based on NEC modeling presented in the preceding sections.

8.3 Comparison of Simulated and Measurement Results

In Chapter 5, we presented the results of two NEC models (M10-3, M15-1) that were based on prototypes (P10-1, P15-1) whose performance was measured and presented in Chapter 7. In this section we compare these simulated and measured results. For detailed information on the models refer to Sections 5.5 and 5.6 as well as Table 5.4. For detailed information on the prototypes refer to Sections 7.3 and 7.4 as well as Table 7.4.

First, we examine the results for the 10-turn SLH prototype (P10-1) which was detailed in Section 7.4 and its corresponding NEC model (M10-3) which was discussed in Section 5.5. For convenience the simulated and measured gain and axial results are plotted together in Figure 8.2.

The measured data for the prototype did not span the entire 3-dB axial ratio bandwidth of the antenna, thus a complete comparison is not possible. However, based on the curves in Figure 8.2 we can draw some conclusions. The operating bandwidth of the NEC model based on the 3-dB axial ratio performance, is shifted up in frequency from that measured in the prototype. The lower edge of the usable bandwidth for the model is 2.55 GHz while the measured lower edge of the bandwidth is 2.4 GHz. The general shape of the axial ratio curve indicates that the NEC model has a upward frequency shift compared to the measured data.

The gain predicted by NEC for this model is higher than that measured in the prototype by 1 dB or more. Also, the measured data indicates that the usable axial bandwidth occurs on the low gain portion of the gain curve, unlike the simulation results.

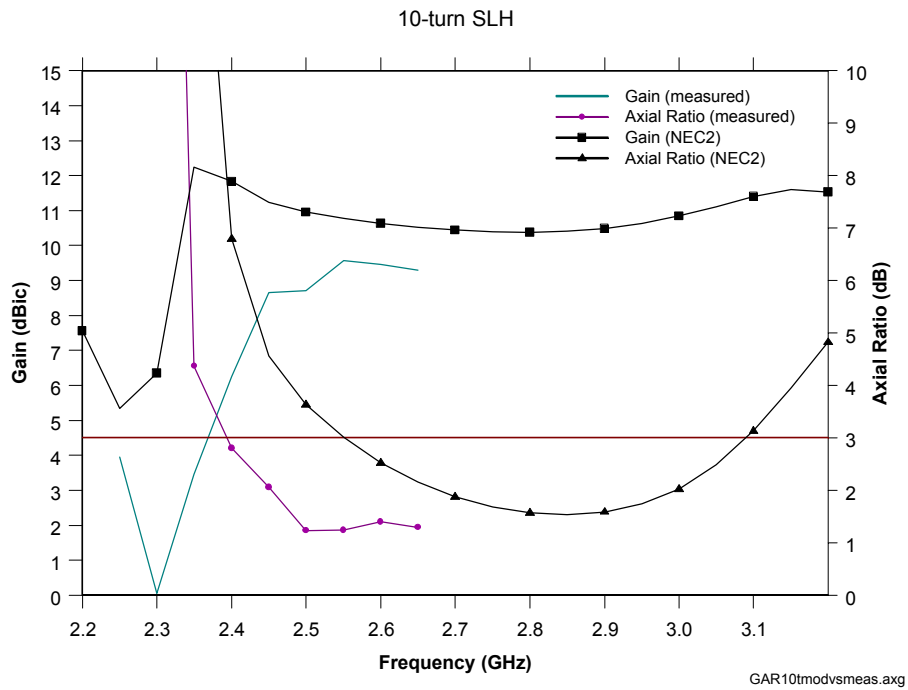


Figure 8.2 Gain and axial ratio measured for 10-turn S-band prototype P10-1 and simulated using NEC for model M10-3.

The measured results from prototype P10-1 are not the best examples for the SLH due to the construction of the prototype. This was a production prototype made with a technique that used a 'fat' winding for the helix. The prototype has rather large stubs and larger than desirable gaps between stub wires; refer to Figure 7.5 for further details. However, the results do indicate that there is a deviation between simulation and measured results.

A second comparison can be made for the 15-turn SLH. Figure 8.3 shows the simulated and measured results for the 15-turn SLH prototype P15-1 and corresponding NEC model M15-1. The measurements here do span the axial ratio bandwidth of the prototype antenna. The axial ratio bandwidth for the NEC model is significantly larger than that measured on the prototype. The model predicted a 3-dB axial ratio bandwidth of 700 MHz. The measured 3-dB axial ratio bandwidth is 270 MHz, only one-third that of the simulation. Again the upward frequency shift of the AR bandwidth of the model from the measured bandwidth is observed in addition to the reduction in bandwidth.

From Figure 8.3 it is observed that the gain predicted through simulation is at least 2 dB or more above the measured gain of the prototype. The general shapes of the gain curves of measured and simulated results are similar, in that both show a significant drop in gain at the upper end of the AR operating bandwidth.

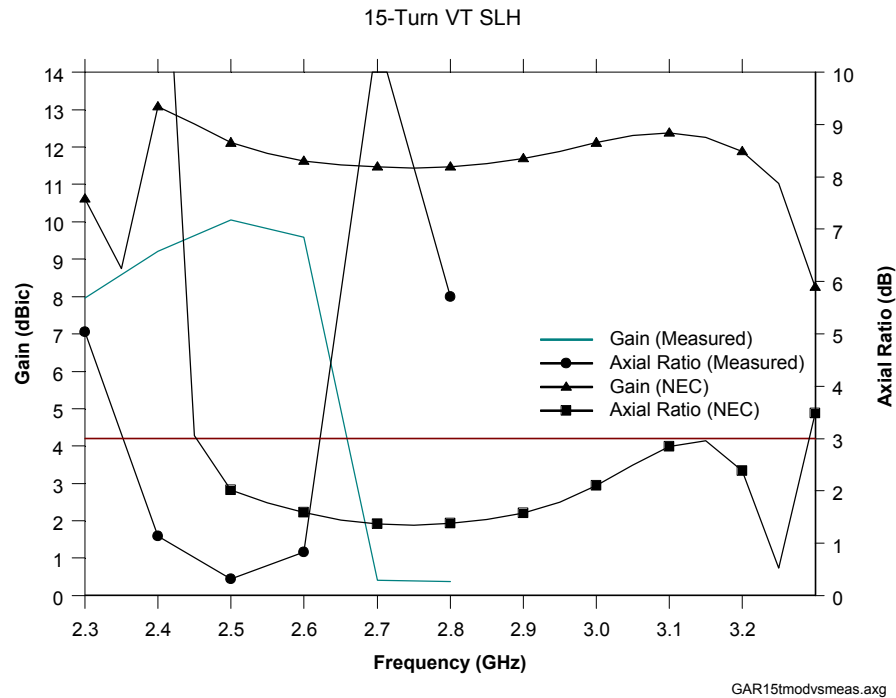


Figure 8.3 Gain and axial ratio measured for 10-turn S-band prototype P15-1 and simulated using NEC model M15-1.

Based on the comparisons shown in Figures 8.2 and 8.3, we can draw some conclusions about the accuracy of NEC modeling of the Stub Loaded Helix antenna. The gain predicted by NEC appears to be at least 1 or 2 dB higher than that realized in the prototypes we examined. The axial ratio bandwidth predicted by NEC is larger, and shifted higher in frequency than that measured in the prototypes discussed (P10-1 and P15-1). This tendency for a frequency shift in the simulated results is also evident in the gain curves in Figures 8.2 and 8.3. In general, we conclude that NEC results are optimistic in predicting gain and axial ratio bandwidth, but are pessimistic in predicting the amount of size reduction, i.e. lowering of operating frequency, produced in the SLH.

The geometry of the SLH is quite complicated and involves many closely spaced wires of relatively short electrical length in the stubs. As with any numerical simulation package, NEC has its limitations and these are generally known. One of these is the difficulty of

dealing with closely spaced wires. Thus, the inaccuracies we have noted in our modeling results may be due in part to our pushing the limits on the capabilities of NEC.

The value of simulation is not in predicting highly accurate absolute values, but rather for use in trade studies involving parameter variations through relative performance evaluation.

8.4 Design Guidelines

Based on the results of NEC simulations and experimental verification of numerous prototype antennas, we developed a simple set of design guidelines for the Stub Loaded Helix antenna. The SLH, much like the conventional axial mode helix, is actually quite tolerant of mechanical inaccuracies in its construction. The helix, both conventional and stub loaded, is an antenna that naturally seems to 'want to work'. However, in order to maximize the performance of the antenna, care must be paid to construction details.

Table 8.2 summarizes the design parameters for the SLH that maximize the gain and axial ratio performance of the antenna while also minimizing the size of the helix. As discussed in Chapter 6, the simulation results indicated that the optimal number of stubs-per-turn, N_s , for maximum size reduction was six, but this entailed a slight reduction in axial ratio bandwidth. An N_s value of four maximized the axial ratio bandwidth of the antenna and also simplifies the mechanical complexity of its construction.

Table 8.2 Optimum SLH Design Parameters for Maximizing Gain and Axial Ratio

C, circumference	$0.75 \lambda_c$
R, radius	$0.119 \lambda_c$
α , pitch angle	8°
N_s , # stubs-per-turn	4
l_s , stub depth	$0.666R - 0.75R$

The one detail of construction that is not obvious is the construction of the stubs. Problems associated with the modeling of the stubs was mentioned in Chapter 5, but little discussion of their construction has been presented except in Chapter 7. In order to minimize any spurious radiation from the stubs, it is imperative that the gap between the two sides of the stub be small. In our handmade prototypes, we used enameled wire and

twisted the stub wires together in order to minimize the gap as well as provide for some additional mechanical support for the stubs. The enamel coating provided insulation and prevented the stub from electrically shorting out. It is not necessary to go to this extreme, but the smaller the gap between the sides of the stubs, the better. An excessively large gap usually results in a reduction in gain and/or axial ratio bandwidth.